Neutron matter at low density and the unitary limit

M. Baldo and C. Maieron
Dipartimento di Fisica, Università di Catania and INFN, Sezione di Catania Via S. Sofia 64, I-95123, Catania, Italy
(Received 15 October 2007; published 3 January 2008)

Neutron matter at low density is studied within the hole-line expansion. Calculations are performed in the range of Fermi momentum k_F between 0.4 and 0.8 fm^{-1}. It is found that the Equation of State is determined by the $^1S_0$ channel only, the three-body forces contribution is quite small, the effect of the single particle potential is negligible and the three hole-line contribution is below 5% of the total energy and indeed vanishing small at the lowest densities. Despite the unitary limit is actually never reached, the total energy stays very close to one half of the free gas value throughout the considered density range. A rank one separable representation of the bare NN interaction, which reproduces the physical scattering length and effective range, gives results almost indistinguishable from the full Brueckner G-matrix calculations with a realistic force. The extension of the calculations below $k_F = 0.4$ fm^{-1} does not indicate any pathological behavior of the neutron matter equation of state.

DOI: 10.1103/PhysRevC.77.015801 PACS number(s): 21.65.−f, 24.10.Cn, 26.60.−c, 03.75.Ss

I. INTRODUCTION

The crust of neutron stars is composed of a solid lattice of nuclei, whose masses and neutron excess increase as one proceeds from the surface to the interior [1]. This is due to the increase of the matter density and of the corresponding electron density, which shifts the beta equilibrium toward larger and larger nuclear asymmetry. At a definite density nuclei start to drip neutrons since their chemical potential turns positive. The inner crust is then formed by a nuclear lattice permeated by a gas of neutrons. From the drip point on, the neutron gas density increases, starting in principle from a vanishing small value, up to the point where nuclei merge and possibly form more complicated structures and finally a homogeneous matter of neutrons and protons appears. This is one of the main reasons of the great interest that has been devoted to the study of the equation of state (EOS) of pure neutron matter. The low density region is less trivial than one could expect at a first sight since the neutron-neutron scattering length is extremely large, about −18 fm, due to the well known virtual state in the $^1S_0$ channel, and therefore even at very low density one cannot assume the neutrons to be uncorrelated. These considerations have also stimulated a great interest in the so called unitary limit, i.e., the limit of infinite (negative) scattering length of a gas of fermions at vanishing small density. A series of works [2–4] have been presented in the literature based on various approximations and a recent Monte Carlo calculation [5] on a related physical system has shown that the unitary limit can present a quite complex structure, involving both fermionic and bosonic effective degrees of freedom, which has still to be elucidated. Variational [6] and finite volume Green's function Monte Carlo calculations [7] for neutron matter at relatively low density have shown that the EOS, in a definite density range, can be written as the free gas EOS multiplied by a factor ξ, which turns out to be close to 0.5. This is actually what one could expect in the unitary limit regime, since no scale exists in this case, except the Fermi momentum. Monte Carlo calculations [2–4] with schematic forces in a regime close to the unitary limit have found a factor $\xi \approx 0.44$. The connection between the variational results and the unitary limit has been studied in Ref. [8] by means of effective theory methods.

In this paper we present results on pure neutron matter EOS based on the hole-line expansion of Bethe, Brueckner, and Goldstone (BBG) [9], which is particularly suited for the low density regime. We use a realistic force, as specified below, and we show that at the lowest density a rank one separable representation of the neutron-neutron interaction, which incorporates the physical values of the scattering length and effective range, is able to reproduce accurately the EOS obtained with the full glory NN interaction. The extension of the calculations to very low density is also discussed.

II. THE IN MEDIUM G-MATRIX

Since the scattering length a and effective range r_0 in the $^1S_0$ channel of the neutron-neutron interaction differ by about a factor 6, there is no density interval where the unitary limit can be considered strictly valid. However, in the range $r_0 < d < |a|$, where d is the average interparticle distance, the physical situation should be the "closest" possible to the unitary limit. For the sake of comparison we first restrict the analysis to the density range corresponding to 0.4 fm^{-1} $< k_F <$ 0.8 fm^{-1}, which falls in this range and corresponds to densities between about 1/50 and 1/5 of the saturation density. As a modern realistic nucleon-nucleon potential we choose the Argonne v_{18} interaction [10]. From the three-body force of the Urbana model, adjusted to reproduce the correct saturation point [11], we found a contribution which is less than 0.01 MeV, and therefore we neglect three-body forces hereafter.

The basic quantity in the BBG expansion is the Brueckner G-matrix, which satisfies the integral equation

$$\langle k_1k_2|G(\omega)|k_3k_4\rangle = \langle k_1k_2|v|k_3k_4\rangle + \sum_{k_3'k_4'}\langle k_1k_2|v|k_3'k_4'\rangle \times \frac{(1-\Theta_F(k_3'))(1-\Theta_F(k_4'))}{\omega - e_{k_3'} - e_{k_4'}} \times \langle k_3'k_4'|G(\omega)|k_3k_4\rangle. \quad (1)$$

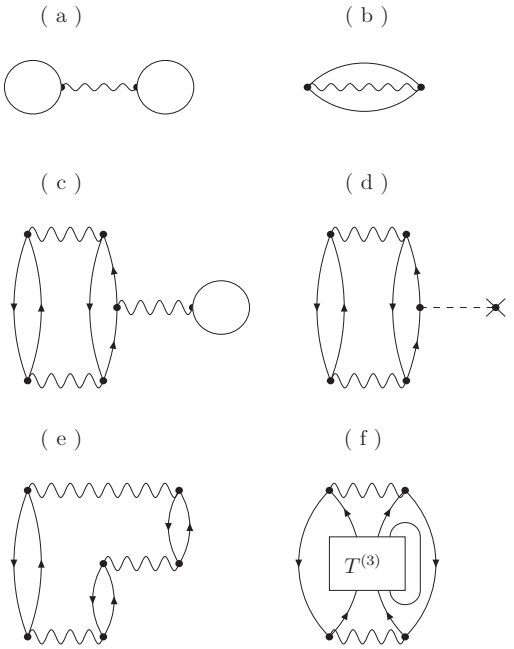

FIG. 1. Two and three hole-line diagrams for the ground state energy in terms of the G-matrix (wiggly lines).

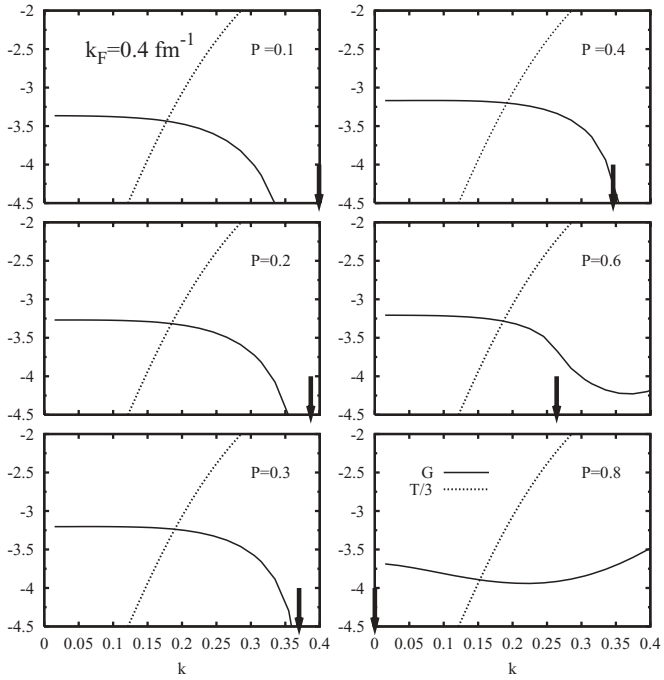

FIG. 2. Comparison between the free T-matrix and the Brueckner G-matrix at different total momentum P and relative momentum k (in fm^{-1}) at the Fermi momentum $k_F = 0.4$ fm^{-1}. The arrows indicate the upper limit of the momentum integration needed for calculating the interaction energy.

The intermediate states are particle states, and this is indicated in Eq. (1) by the two Pauli projection factors $1 - \Theta_F(k)$, being $\Theta_F(k)$ the Fermi distribution at zero temperature. The entry energy ω is specific of each diagram where the G-matrix appears. At the two hole-line level of approximation, the diagrams which contribute are the ones indicated by labels (a) and (b) in Fig. 1 (first row), where the wiggly line indicates the Brueckner G-matrix.

They correspond to the Brueckner-Hartree-Fock (BHF) approximation. For these diagrams the entry energy is just the energy of the two interacting particles. It is remarkable that even at the relatively low densities we are considering the inclusion of the Pauli projection in the intermediate states produces the overwhelming dominant in medium effect. This is illustrated in Fig. 2, where the diagonal G-matrix in the $^1S_0$ channel is reported in comparison with the corresponding free T-matrix (divided by 3) at selected values of the relative momentum k and total momentum P (in fm^{-1}) at the Fermi momentum $k_F = 0.4$ fm^{-1}.

Of course, due to Galilei invariance, the free T-matrix is independent of P. For simplicity the free single particle spectrum (kinetic energy) is adopted in these calculations, but, as we will see, this is not a serious restriction. Despite the Fermi momentum is quite small, a drastic difference between the two scattering matrices is apparent, not only in shape but also in absolute value. The Pauli operator effect is enhanced in this particular channel since the virtual state is suppressed in the medium, as we will discuss later in detail. The arrows indicate the upper limit of the momentum integration needed for calculating the interaction energy. To be noticed is also the pairing singularity at the Fermi momentum and for small total momentum P. This singularity is integrable and can be handled without numerical problems. This means of course that we are neglecting the pairing condensation energy, which is however negligible in this density range. In any case we are going to compare in a coherent fashion only calculations that neglect the pairing contribution.

Since s-wave dominates at low density, the in medium modification of the G-matrix in the $^1S_0$ channel has a profound and essential effect on the EOS. Indeed, higher partial waves give a negligible contribution to the interaction energy. In practice the calculation of the EOS at the BHF level of approximation reduces to a single channel problem in the considered density range (or below). The inclusion of higher partial waves would not alter at all our analysis and conclusions.

In the BBG expansion an auxiliary single particle potential $U(k)$ is introduced. Then the single particle energy reads

$$e(k) = \frac{\hbar^2 \mathbf{k}^2}{2m} + U(k) \tag{2}$$

and the potential $U(k)$ is determined in a self-consistent way in terms of the Brueckner G-matrix

$$U(k) = \sum_{k' < k_F} \langle kk' | G\big(e_{k_1} + e_{k_2}\big) | kk' \rangle, \tag{3}$$

The auxiliary potential is essential to get convergence in the BBG expansion [9,12]. However in the low density regime we are considering we found that its effect on the G-matrix is negligible, at least within the accuracy we need for the considerations developed in the present work. This does not mean that we can neglect $U(k)$ altogether, since, as we will see, at the three hole-line level of approximation its effect through the "U-insertion" diagram is of some relevance.

III. THE THREE HOLE-LINE CONTRIBUTION AND THE EOS

The BBG expansion relies on the basic idea that the contributions of the diagrams of the expansion decrease with increasing number of hole-lines which are included. Despite that BBG is essentially a low density expansion, it has been found [13,14] that the convergence is valid up to densities as high as few times saturation density in symmetric nuclear matter and even better in neutron matter. It is then likely that at the low densities we are here considering this convergence should be even faster. This is indeed confirmed by explicit numerical calculations reported below. The three hole-line diagrams can be summed up by means of the Bethe-Fadeev equation [15], which introduces the in medium three-body scattering matrix $T^{(3)}$. It is the analogous for three particles of the in-medium two particle G-matrix. The Bethe-Fadeev integral equation for $T^{(3)}$ is also very similar to the integral equation for the G-matrix, where however in the kernel the G-matrix appears in place of the bare NN interaction. This is in line with the BBG expansion, where the bare NN interaction is systematically replaced by the G-matrix in all the diagrams. In terms of $T^{(3)}$ the contribution to the energy of the three hole-line diagrams can be depicted as in Fig. 1(f), and it includes a direct and an exchange contribution. For numerical convenience the diagrams with three G-matrices only are usually separated from the diagrams with a larger number of G-matrices, which will be indicated as "higher order" three hole-line diagrams. The lower order diagrams are depicted in Fig. 1, together with the U-insertion diagram which contributes at this level of approximation. They are indicated as "bubble diagram" (c), U-insertion diagram (d), and "ring diagram" (e). Diagram (e) can be considered the exchange of diagram (c).

The different three hole-line contributions to the interaction energy are reported in Table I at different densities.

The overall three hole-line diagrams contribution D_3 is positive in this density range and reaches a maximum around $k_F \approx 0.7$ fm^{-1}. This is in line with the calculations at higher density, where D_3 turns actually negative above a certain density. The absolute value of D_3 can be considered small with respect to the two hole-line contribution D_2, but maybe it is not completely negligible. In any case it is regularly decreasing with density and at the lowest densities it becomes indeed negligible. As it is well known from previous calculations, at densities higher than the ones considered here, the smallness of D_3 is the result of a strong compensation among the different contributions. While the "higher order" terms, as defined above, can safely be considered negligible, the absolute values of the bubble and U-insertion diagrams, and, to a less extent, also the ring diagram are individually not negligible, but their cancellation reduces by a large factor their overall contribution. The smooth variation of each of these diagrams with density makes the full three hole-line contribution decrease by almost one order of magnitude from the highest to the lowest density.

We take this result as an indication of the convergence of the BBG hole-line expansion and we will assume in the following that the total contribution of the diagrams with a number of hole-lines larger than three can be neglected. To this respect it has to be noticed that the bubble and U-insertion diagrams have opposite sign and their absolute values must become closer and closer at lower density. In fact their absolute values are not equal because the G-matrix of the bubble diagram is "off shell," while the the G-matrix which defines the potential $U(k)$ of Eq. (3), as appearing in the U-insertion diagram, is "on shell". In other words the entry energies of the two G-matrices, which are attached to the particle line on the right in Fig. 1(c) and in Fig. 1(d), are different in the two diagrams. However, it can be easily seen that the difference between these two entry energies is a quantity proportional to the Fermi energy, and therefore vanishing small at low enough density. The cancellation is therefore expected and clearly apparent from the results of the explicit calculations. It can be concluded that the three hole-line contribution further down in density can be safely neglected.

TABLE I. Three hole-line contributions to the neutron matter EOS. D_3 is the total three hole-line contribution, B is the "bubble diagram" of Fig. 1(c), BU is the U-insertion diagram of Fig. 1(d), R is the "ring diagram" of Fig. 1(e), and H indicates the "higher order" diagrams, as defined in the text. Energies are in MeV.

k_F (fm^{-1})	D_3	B	BU	R	H
0.4	0.023	−0.630	0.485	0.156	0.012
0.5	0.091	−0.416	0.389	0.122	−0.004
0.6	0.107	−0.526	0.515	0.123	−0.005
0.7	0.153	−0.611	0.648	0.121	−0.005
0.8	0.148	−0.592	0.651	0.095	−0.006

IV. DISCUSSION

In the BBG expansion the EOS is given by the sum of the free kinetic energy and the interaction energy discussed above. It is reported in Fig. 3, where we also show the neutron matter EOS estimated in Ref. [8] and the variational calculation of

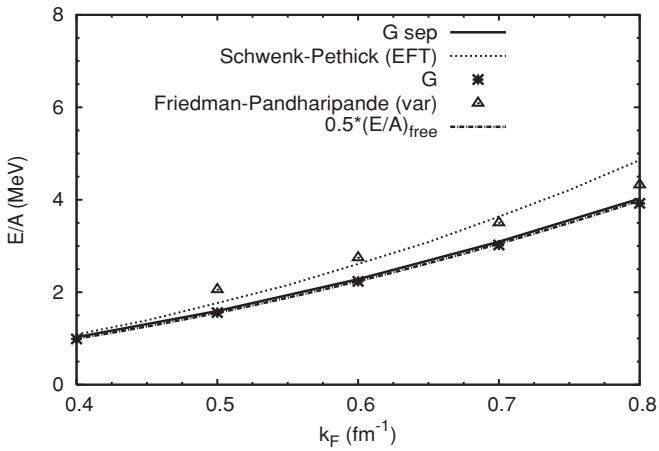

FIG. 3. Neutron matter EOS calculated within the BBG method (label G), within the variational method of Ref. [6] (triangles), according to the estimate of Ref. [8] (dotted line) and with the separable representation of the G-matrix (label G sep). The dash-dotted line is one-half of the free gas EOS.

Ref. [6]. The contribution of the three hole-line diagrams is hardly visible in the plot and it is neglected.

For comparison we also report the value of the free kinetic energy divided by a factor 2. As already noticed in Ref. [7], these values stay surprisingly close to the full microscopic EOS. The agreement seems to indicate that indeed the total energy is a function only of the Fermi momentum k_F, as expected in the unitary limit. In the latter case, however, Monte Carlo calculations [2–4] suggest a factor 0.44 rather than the value 0.5 found in our calculations. As noticed previously, the unitary limit is not actually valid in neutron matter and the reason of such an agreement must be found in some other more general considerations. To clarify this point we take advantage on the above described results that the EOS is determined to a good accuracy only by the G-matrix in the $^1S_0$ channel calculated with the free single particle spectrum. We then construct a rank one separable representation of the bare interaction which gives a free T-matrix, also separable, with the known scattering length and effective range of the neutron-neutron interaction in this channel and it actually depends only on these two physical quantities. The corresponding in-medium G-matrix will be also separable and will depend in addition on the Fermi momentum. If we take, for simplicity, a Laurentzian form factor

$$\phi(k) = 1/(k^2 + b^2) \tag{4}$$

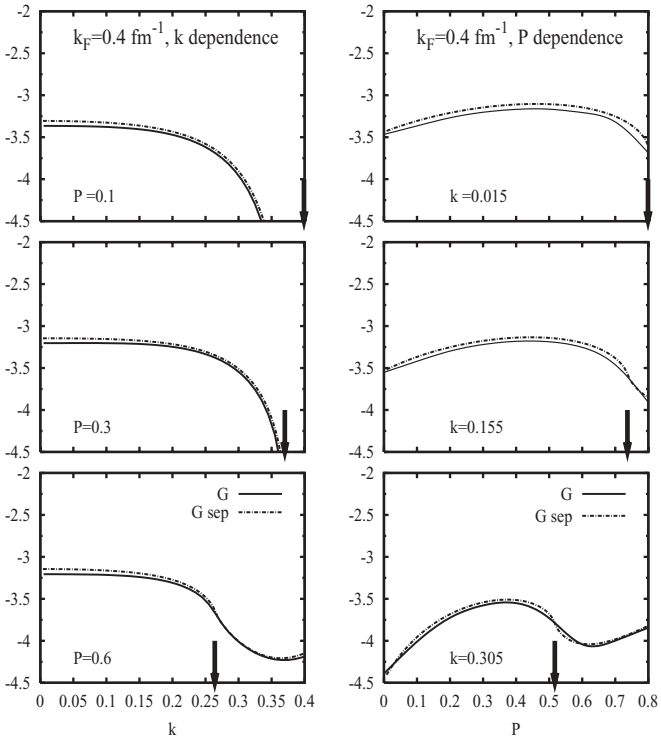

FIG. 4. Diagonal on shell G-matrix (full line) and the corresponding separable representation (dot-dashed line) at selected values of the total momentum P and relative momentum k and at the Fermi momentum $k_F = 0.4$ fm^{-1}. The arrows have the same meaning as in Fig. 2.

to be used for the bare neutron-neutron interaction, the diagonal on-shell T-matrix can be written

$$\langle k|T|k\rangle = a/[1 + u(u + 2 - \beta)/(1 + \beta)], \tag{5}$$

where $u = k^2/b^2$ and the parameters b and β are determined by the relationships

$$a = \frac{1}{b}\left(\frac{2\beta}{1+\beta}\right); \quad r_0 = \frac{1}{b}\left(\frac{\beta-2}{\beta}\right). \tag{6}$$

The values $a = -18.5$ fm and $r_0 = 2.7$ fm are used in the present calculation. More details can be found in the Appendix. For large enough values of b, i.e., small value of r_0, the separable representation is physically equivalent to a zero range interaction with a smooth cutoff. However, the representation is valid in the general case. In principle the effective range expansion holds at small values of the momentum k, more precisely for $k^2 \ll (ar_0)^{-1}$. However, if the scattering is dominated by the virtual state of the neutron-neutron $^1S_0$ channel, the separable representation can be valid in a wider range of momenta. The function $\phi(k)$ can be then interpreted as the form factor for the quasibound state (which is actually related to the corresponding Gamow state [16,17]).

The in-medium G-matrix corresponding to the separable representation can be written as in Eq. (5), where however in the denominator an additional term appears, whose explicit expression is given in the Appendix. The accuracy of the separable representation can be appreciated in Figs. 4, 5, and 6, where the exact (full line) and separable (dashed line) diagonal on-shell G-matrices at different densities and momenta are compared. The arrows have the same meaning as in Fig. 2.

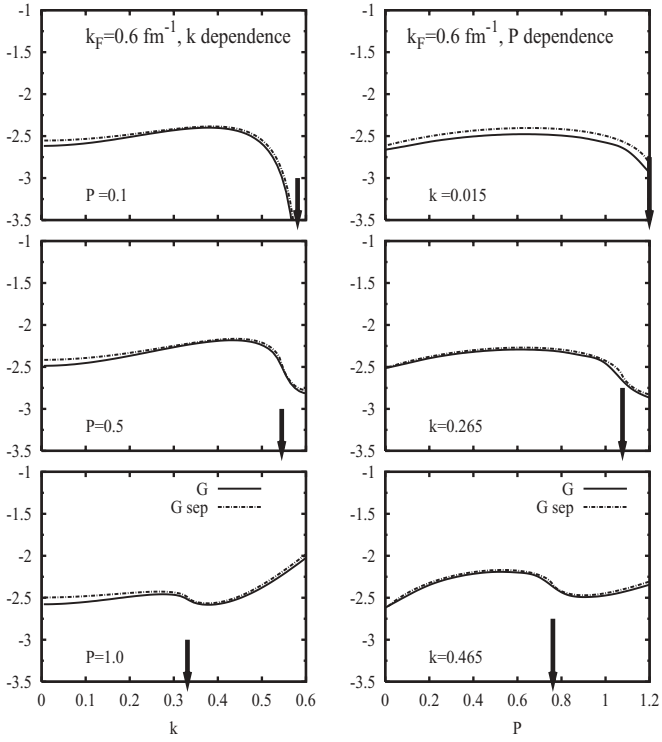

FIG. 5. Same as in Fig. 4, but at $k_F = 0.6$ fm^{-1}.

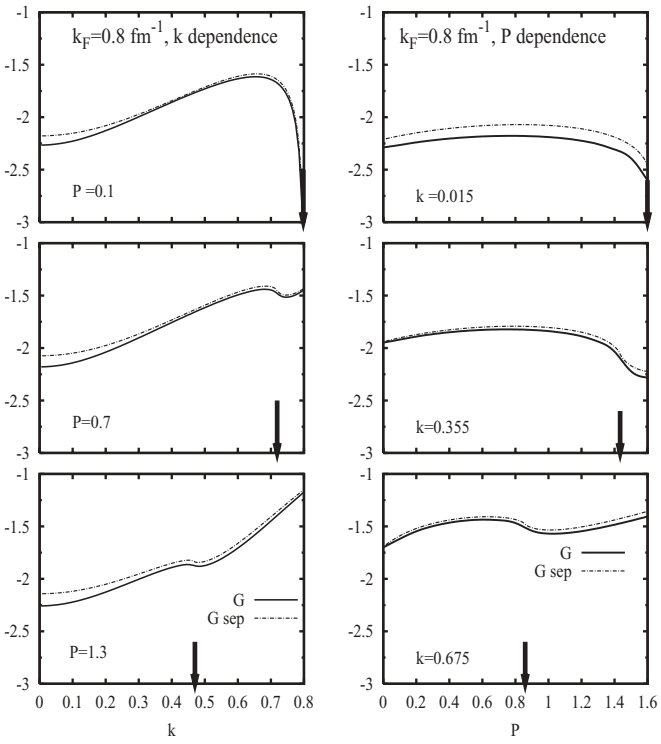

FIG. 6. Same as in Fig. 4, but at $k_F = 0.8$ fm^{-1}.

As expected, no virtual state is present for the G-matrix and correspondingly the in-medium scattering length is strongly modified. As argued in Ref. [7], it becomes of order k_F^{-1}, while the effective range is substantially reduced (see Appendix). Since the phase space present in the calculation of the interaction energy is proportional to k_F^3, this can be a possible explanation of the k_F^2 dependence of the binding energy per particle [7], despite neutron matter is not strictly in the unitary limit regime. The reduction of the total energy with respect to the free gas value E_{FG} by a factor so close to 2 is of course not easy to explain in simple terms. The EOS calculated with the separable G-matrix is reported in Fig. 3. It is indistinguishable with respect to the calculation with the exact G-matrix. This shows that the bare interaction is mainly determined by the virtual state (as embodied in the scattering length and effective range values) and its in-medium suppression is the mechanism which supersedes at the neutron matter EOS in the low density regime.

In Fig. 3 we also report the EOS obtained within the variational method in Ref. [6] as well as the result of the approximate estimate of Ref. [8], based on effective theory methods. Some discrepancy is present at the higher densities, but all the EOS seem to converge closely at the lower densities, maybe with the variational results slightly apart. Actually the variational calculation was performed with a different bare interaction, the Urbana v_{14} [6]. However, we checked that the EOS calculated within the BBG method with this different interaction is indistinguishable from the one reported in Fig. 3. This is in line with the fact that the interaction is determined solely by the scattering length and the effective range, as the present analysis with the separable interaction

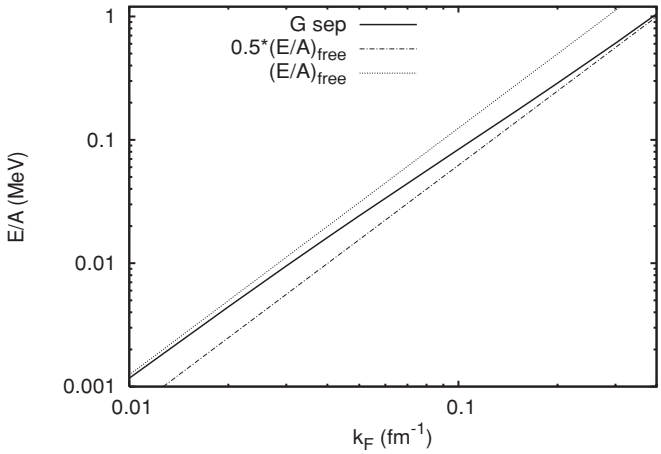

FIG. 7. Neutron matter EOS compared with the free gas one E_{FG} and with $E_{FG}/2$.

clearly indicates. The discrepancy is therefore not due to the different interactions used but to the different adopted many-body methods. The variational results are indeed slightly above the BBG results.

On the basis of the results of our analysis, it is possible to extend the calculation of the EOS below $k_F = 0.4$ fm^{-1}, just by using only the separable G-matrix, since then the separable representation is even more accurate. In Fig. 7 the EOS is reported in comparison with $\frac{1}{2}E_{FG}$.

One can see that deviations start now to appear, which indicates that the simple rule of a factor $1/2$ is valid only in a limited range of density, where indeed the neutron matter is "closest" to the unitary limit. Indeed the deviations start to appear for $k_F r_0 < 1$. Outside the considered range $0.4 < k_F < 0.8$ fm^{-1} the total energy is not $\frac{1}{2}E_{FG}$ and even not proportional to k_F^2. At decreasing density the EOS is merging into the free gas EOS, but this happens only at extremely low values, approximately in agreement with the condition $k_F|a| \ll 1$. At these very low density pairing could be of some relevance, but it cannot affect appreciably the total energy since, once again, the unitary limit is not reached.

V. CONCLUSIONS

In this paper we have established the pure neutron matter EOS on the basis of the BBG many-body theory. We found that the EOS is determined with high accuracy by the G-matrix in the $^1S_0$ channel only. In the range of density corresponding to the Fermi momenta $0.4 < k_F < 0.8$ fm^{-1} the EOS turns out to be very close to the value $\frac{1}{2}E_{FG}$, where E_{FG} is the free Fermi gas EOS. In this density range the condition $1/|a| < k_F/\alpha < 1/r_0$ is satisfied, with $\alpha = 2(9\pi/4)^{\frac{1}{3}}$ and α/k_F is the average distance between particles. Here the scattering length a and the effective range r_0 are the ones of the $^1S_0$ neutron-neutron channel. We interpret this results as an indication that neutron matter in this density range is in some way "close" to the unitary limit, even if such limit is strictly not reached. In fact, for the unitary limit Monte Carlo calculations [2–4] predict that the corresponding EOS should be approximately $0.44E_{FG}$.

A rank one representation of the neutron-neutron interaction, which is determined only by the scattering length and effective range, proves to be extremely accurate in reproducing the G-matrix and the EOS. Below $k_F = 0.4$ fm^{-1} the EOS is not given by $\frac{1}{2}E_{FG}$ and in the low density limit, when $k_F|a| \ll 1$, it approaches smoothly the free gas E_{FG}. Above $k_F = 0.8$ fm^{-1} the EOS is not any more dominated by the s-wave part of the NN interaction. As more complete calculations have shown [13,14], in this case the EOS has no simple behavior.

APPENDIX

In this appendix we give some details about the separable form of the neutron-neutron interaction in the $^1S_0$ channel and the corresponding in-medium G-matrix suitable in the low density region as discussed in the paper. The rank-one representation of the interaction is written as

$$(k'|v|k) = \lambda\phi(k')\phi(k), \tag{A1}$$

where the form factor $\phi(k)$ is given by Eq. (4). The corresponding scattering T-matrix in free space can be evaluated following the standard procedure for separable interactions

$$(k'|T(\omega)|k) = \lambda\phi(k')\phi(k)/[1 - \langle\phi|G_0(\omega)|\phi\rangle], \tag{A2}$$

where G_0 is the free Green's function and ω is the entry energy. With our choice of the form factor the integral for evaluating the matrix element of the denominator can be performed analytically. The separable interaction and the corresponding T-matrix depend only on the two parameters λ and b. Expanding the diagonal ($k' = k$) T-matrix for low momenta and on-shell, i.e., at the kinetic energy $\omega = k^2/2\mu$, one can relate these two parameters to the scattering length a and effective range r_0 of the original neutron-neutron interaction. This finally gives Eq. (6) and the expression for the T-matrix in Eq. (5).

Going to the in-medium G-matrix, one has simply to modify the integral for the evaluation of the matrix elements of the free Green' s function by restricting the integration above the Fermi surface. Still the integral can be done analytically, and the final expression reads

$$(k|G(P,k_F)|k) = 1\Big/\Big[\big(1/a - \tfrac{1}{2}r_0k^2 + \tfrac{1}{2}k^4\big/(b^3\beta)\big) + A(k,P,k_F)\Big]. \tag{A3}$$

Neglecting the term $A(k, P, k_F)$ in the denominator, one recovers the free T-matrix of Eq. (5). The medium effects are embodied in A, which reads

$$\begin{aligned} A = &-\frac{1}{\pi b}(b^2 - k^2)\arctan\left(\frac{k_F + P/2}{b}\right) \\ &+\frac{1}{\pi}k\log\left(\frac{k + k_F + P/2}{-k + k_F + P/2}\right) + \frac{1}{\pi P}\left(k_F^2 - P^2/4 - k^2\right) \\ &\times\log\left|\frac{(k_F + P/2)^2 + b^2}{k_F^2 - P^2/4 + b^2}\cdot\frac{k_F^2 - P^2/4 - k^2}{(k_F + P/2)^2 - k^2}\right|, \end{aligned} \tag{A4}$$

where P is the total momentum of the two particles. Expanding the G-matrix at small momentum and at $P = 0$, one can obtain the in-medium scattering length a' and effective range r_0'. They read

$$a' = a\Big/\left(1 - \frac{ab}{\pi}\arctan\left(\frac{k_F}{b}\right)\right) \approx -\frac{\pi}{2k_F}; \tag{A5}$$

$$r_0' \approx r_0 - \frac{4}{\pi k_F}. \tag{A6}$$

The expression for r_0' is obtained assuming $k \ll k_F$, so it cannot be considered at too low density.

[1] S. L. Shapiro and S. A. Teukolsky, *Black Holes, White Dwarfs and Neutron Stars* (John Wiley and Sons, New York, 1983).
[2] J. Carlson, S.-Y. Chang, V. R. Pandharipande, and K. E. Schmidt, Phys. Rev. Lett. **91**, 050401 (2003).
[3] G. E. Astrakharchik, J. Boronat, J. Casulleras, and S. Giorgini, Phys. Rev. Lett. **93**, 200404 (2004).
[4] A. Bulgac, J. E. Drut, and P. Magierski, Phys. Rev. Lett. **96**, 090404 (2006).
[5] A. Bulgac, J. E. Drut, and P. Magierski, Phys. Rev. Lett. **99**, 120401 (2007).
[6] B. Friedman and V. R. Pandharipande, Nucl. Phys. **A361**, 501 (1981).
[7] J. Carlson, J. Morales, V. R. Pandharipande, and D. G. Ravenhall, Phys. Rev. C **68**, 025802 (2003).
[8] A. Schwenk and C. J. Pethick, Phys. Rev. Lett. **95**, 160401 (2005).
[9] For a pedagocical introduction see *Nuclear Methods and the Nuclear Equation of State*, edited by M. Baldo (World Scientific, Singapore, 1999).
[10] R. B. Wiringa, V. G. J. Stoks, and R. Schiavilla, Phys. Rev. C **51**, 38 (1995).
[11] M. Baldo, I. Bombaci, and G. F. Burgio, Astron. Astrophys. **328**, 274 (1997); X. R. Zhou, G. F. Burgio, U. Lombardo, H.-J. Schulze, and W. Zuo, Phys. Rev. C **69**, 018801 (2004).
[12] M. Baldo and C. Maieron, J. Phys. G: Nucl. Part. Phys. **34**, R243 (2007).
[13] M. Baldo, C. Maieron, P. Schuck, and X. Vinas, Nucl. Phys. **A736**, 241 (2004).
[14] M. Baldo, A. Fiasconaro, H. Q. Song, G. Giansiracusa, and U. Lombardo, Phys. Rev. C **65**, 017303 (2001).
[15] R. Rajaraman and H. A. Bethe, Rev. Mod. Phys. **39**, 745 (1967).
[16] G. Gamow, Z. Phys. **51**, 204 (1928).
[17] M. Baldo, L. S. Ferreira, and L. Streit, Phys. Rev. C **32**, 685 (1985).